structure interaction aspects but appears, however, to be conservative.

The performance of the structure at Monessen provided a valuable test case for the adequacy of the current design practice because the structure supported the slope above it despite the unexpected slope failure below.

## CONCLUSIONS AND RECOMMENDATIONS

Based on the experience with and the available structure-movement data from this project, the following conclusions are made:

1. The root-pile structure provides a fast and economical alternative to many conventional structures.
2. Before the installation of the root piles, the movements of the cap beam varied from less than 2.5 cm at the north end to more than 46 cm at the south end. These movements were due to movements of unstable soil in the slide area.
3. After the installation of the root piles, there were significant movements [up to 5 cm (2 in)] in the cap beam as well as in the soil below it. This indicates that some movement of the root-pile structure was needed before resistance to earth pressure could be mobilized.
4. No significant soil movement through the root piles could be detected; i.e., the small-diameter piles and the soil between them appeared to work as a single composite structure.
5. The construction of the root-pile wall was rapid and caused little or no disturbance to the existing terrain.
6. Conventional design procedures for retaining walls appear to provide overall design for root-pile walls. The geometry of the root-pile structure described in this paper is patented and may not be the optimum design for all situations. Therefore, the design procedure for the geometry and size of the individual piles within the root-pile structure should be investigated further. A rational method, one that considers soil-structure interaction, should be developed for the design of root-pile structures and verified by using actual field measurements of prototype construction.
7. There should be more test cases of root-pile construction; the instrumentation should be adequate to measure loads and movements so that the design methods can be evaluated.

## ACKNOWLEDGMENT

The construction of this root pile was carried out under the supervision of Engineering District 12 of the Pennsylvania Department of Transportation. William R. Galanko and William T. Mesaros of the district provided assistance throughout the duration of the project. The help of Donald L. Keller, Phillip E. Butler, Kenneth J. Rush, and others in the Bureau of Materials, Testing, and Research is appreciated. We also thank the Ram Construction Company, the general contractor for the project, and the Fondedile Corporation of Boston, Massachusetts, who did most of the root-pile wall construction work.

## REFERENCES

1. F. Lizzi. Special Patented Systems of Underpinning and Root Piles with Special Reference to Problems Arising from the Construction of Subways in Built-up Areas. Fondedile Corp., Boston, MA, 1972.
2. Fondedile System. Fondedile Corp., Boston, MA, no date.
3. F.A. Bares. Use of Pali Radice (Root Piles) for the Solution of Difficult Foundation Problems. Presented at ASCE Transportation Engineering Meeting, Montreal, July 1974, Preprint MTL-41.
4. Fondedile Corp. Root-Pattern Piles Underpinning. Proc., Symposium on Bearing Capacity of Piles, Central Building Research Institute, Roorkee, India, Feb. 1964.

*Publication of this paper sponsored by Committee on Embankments and Earth Slopes.*

# Analysis of an Earth-Reinforcing System for Deep Excavation

S. Bang, C. K. Shen, and K. M. Romstad

**A limit-analysis procedure for a reinforced lateral earth support system is described. The system is composed of a wire-mesh-reinforced shotcrete panel facing, an array of reinforced anchors grouted into the soil mass, and rows of reinforcing bars that form horizontal wales at each anchor level. Excavation starts from the ground level and, after each layer, reinforcement is applied immediately on the exposed surface and into the native soil. This system thus forms a temporary earth support that has the advantages of requiring no pile driving, not loosening or sloughing the soil, and providing an obstruction-free site for foundation work. It has been successfully used for large areas of excavation to depths of up to 18 m in various ground conditions. However, in the past, no rational and proven analytical design procedure was available, a problem that resulted in considerable reservation toward the use of the system among engineers and contractors. The two-dimensional plane-strain limit-analysis formulation includes consideration of design parameters such as soils type, depth of excavation, length of the reinforcing members, inclination, and spacing. The analysis procedure can be used to evaluate the overall stability of the system and to determine the proper size, spacings, and length of the reinforcement for a given site condition.**

In recent years, underground construction has been widely used as a logical part of the solution to many urban and city problems. Sewer and water conduits and other utility lines are usually installed underground in large cities, and vehicular tunnels and underground stations can decrease both intracity and intercity traffic congestion and thus improve both air quality and traffic safety. Even more important is that increased underground building construction is a desirable alternative that saves energy. To meet the challenge of increasing demand, it is imperative that effective, economical, and safe underground excavation technology be developed.

This paper describes a limit-analysis procedure for a relatively new, reinforced lateral earth support system for deep excavation. This system has been used in Vancouver, British Columbia, in Edmonton, Alberta, and more recently in Portland, Oregon (1), to depths up to 18 m. Varying ground conditions have been encountered, including sandy and clayey fills, glacial tills, sandy and silty alluvial deposits, and very soft weathered rocks. The advantages of this system over those of conventional, temporary lateral earth support systems have been reported elsewhere (2, 3). Although the cost of construction is comparable to that of conventional systems, the time required to complete an excavation job can be decreased by 30-50 percent if the new system is used.

Briefly, the system is composed of a 0.1-m-thick, wire-mesh-reinforced shotcrete panel facing; an array of reinforcing members spaced 0.9-1.8 m apart and grouted into the soil mass; and rows of four no. 4 reinforcing bars forming horizontal wales at each anchor level (see Figure 1). Excavation starts at the ground level and, after each layer, reinforcement is applied immediately on the exposed surface and into the native soil. The system offers an unusual way to form a temporary earth support and has the advantages of requiring no pile driving, not loosening or sloughing the soil, and providing an obstruction-free site for foundation work.

## BACKGROUND

Designs for and analyses of this system have usually assumed the classical Rankine's active failure wedge, and the spacing and length of the reinforcing members have been determined by using a procedure similar to the conventional tied-back anchor system design. However, there are some fundamental behavioral differences between the nature of this system and that of other lateral earth support systems. Conventional systems are designed to retain the soil adjacent to a vertical cut,

Figure 1. Typical cross section.

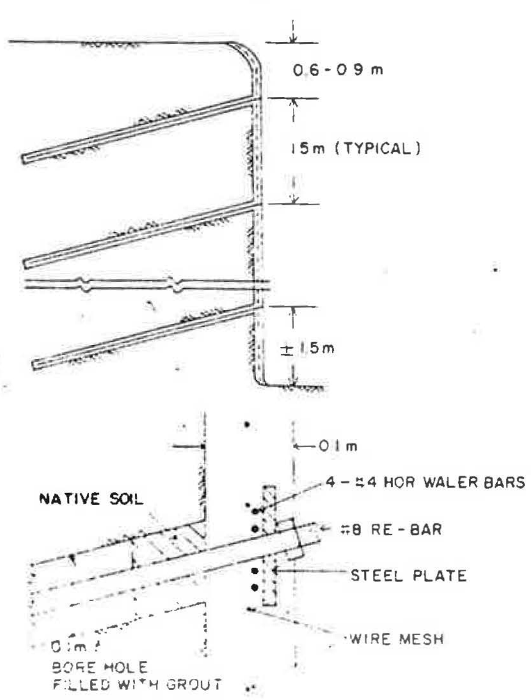


whereas this system is based on strengthening the adjacent native soil so that the system itself can withstand a vertical cut to a depth that normally requires the installation of lateral support. Furthermore, the strengthened soil mass develops its strength through a network of closely spaced reinforcing members that are grouted into the soil. This system can be viewed as a reinforced-earth retaining wall having adequate strength and stability to contain the movement of soil masses both within and behind it.

A simple design method for reinforced-earth walls has been suggested by Lee and others (4) based on the assumption that the classical Rankine's plane failure surface passes through the toe of the wall facing at an angle of $[45 + (\phi/2)]^\circ$ to the horizontal. A similar assumption is made in the method proposed by Holm and Bergdahl (5), which takes into consideration a failure plane having different inclinations and points of intersection with the wall facing.

Although the classical plane failure-surface assumption simplifies the analysis procedure, it is highly unlikely that the failure surface of an adequately designed reinforced-earth wall would give a triangular failure wedge. Laboratory-model tests of reinforced-earth walls (6, 7) have indicated that their failure surfaces are curved and cannot be effectively represented by the conventional plane failure-surface assumption.

Romstad and others (8) approached the design of a reinforced-earth wall by hypothesizing that the failure surface will consist of two planes having a transition at the back edge of the reinforcing strips when it extends beyond the reinforced-earth zone or will be a plane through the toe of the wall when it lies entirely within the reinforced zone.

A similar approach has been used by Smith and Wroth (7). Their hypothesized failure surface is the same as that suggested by Romstad and others. They assume that the resultant of the earth pressure developed between the reinforced and the unreinforced soil blocks forms an angle $\phi$ to the horizontal. The overall stability of the wall is then evaluated by comparing the strip force calculated from the force equilibrium of the reinforced block with the total frictional force calculated from the overburden and the effective strip legnth beyond the assumed failure surface. The disadvantage of this approach is that the factor of safety calculated for a stable reinforced-earth wall is highly unconservative because full friction is assumed to be developed at all times. Therefore, the results are valid only when the wall is on the verge of failure.

## LIMIT ANALYSIS AT EQUILIBRIUM

To date, there have been no prototype failure studies of this new lateral earth support system. Other indirect methods, therefore, must be used to approximate the failure mechanism. As shown in Figure 2, contours of factors of safety can be obtained by a finite-element analysis of the system (9) and, thus, a potential failure surface can be approximated; this potential failure surface passes more or less through the toe of the wall to form a curved surface. As discussed above, most of the proposed design methods for reinforced earth walls (7, 8) approximate this curved failure surface by two planes that have an abrupt change of direction at the back of the reinforced zone. In this analysis, however, it is assumed that the failure surface is more appropriately represented by a parabolic curve passing through the toe of the wall. The parabola can intersect the ground surface at any point by changing the value of "a", as shown in Figure 3. The potential failure surface is then the parabola that has the lowest overall factor of

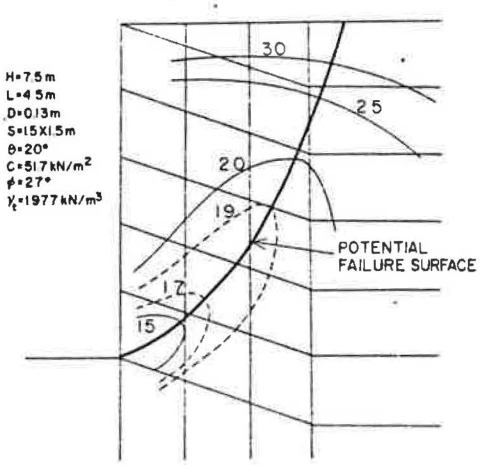

Figure 2. Factor-of-safety contours determined by finite-element analysis.

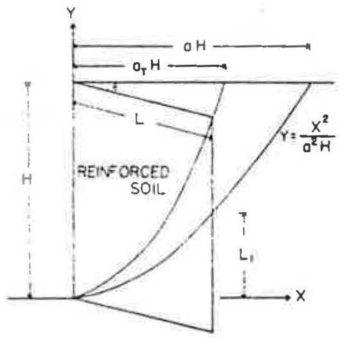

Figure 3. Postulated failure surface: general case.

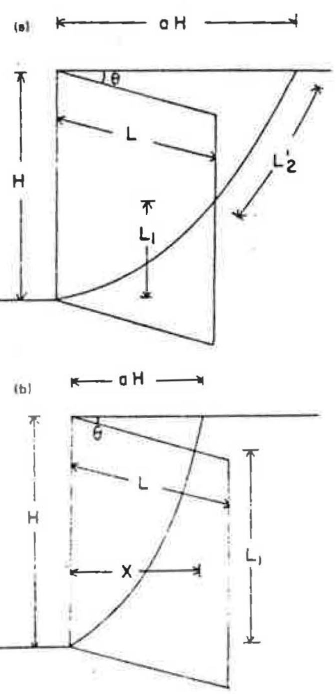

Figure 4. Postulated failure surface: (a) case 1 ($a > a_T$) and (b) case 2 ($a < a_T$).

safety. Two cases must be considered separately: case 1 in which the failure surface extends beyond the reinforced zone and case 2 in which the failure surface lies entirely within the reinforced soil mass (see Figure 4).

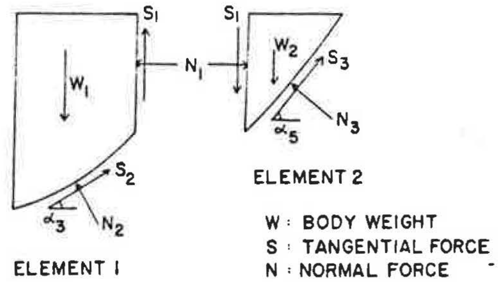

Figure 5. Free-body diagram.

Case 1: $a \geq a_T$.

Figure 5 shows the free-body diagrams of the reinforced soil block (element 1) and the unreinforced soil block (element 2). The directions of the tangential forces acting along the bottom of each element, $S_2$ and $S_3$, are assumed to be parallel to the corresponding chords, i.e.,

$$\alpha_3 = \tan^{-1}(L_1/L\cos\theta) \tag{1a}$$

$$\alpha_5 = \tan^{-1}(H - L_1)/(aH - L\cos\theta) \tag{1b}$$

where

$$L_1 = y\big|_{x = L\cos\theta} = L^2\cos^2\theta/a^2H \tag{2}$$

The equilibrium equations of element 1 are thus

$$N_2 = (W_1 - S_1)\cos\alpha_3 - N_1\sin\alpha_3 \tag{3}$$

$$S_2 = (W_1 - S_1)\sin\alpha_3 + N_1\sin\alpha_3 \tag{4}$$

where

$$W_1 = HL\gamma\cos\theta - \int_0^{L\cos\theta}(x^2/a^2H)\gamma dx$$

$$= \gamma\,[HL\cos\theta - (L^3\cos^3\theta/3a^2H)] \tag{5}$$

$S_1 = \beta N_1$ (i.e.,
$\beta$ = ratio of $S_1$ to $N_1$),
$N_1 = \frac{1}{2}K\gamma(H - L_1)^2$,
$\alpha$ = unit weight of soil, and
$K$ = stress ($\sigma$) ratio = $\sigma_h/\sigma_v$.

The equilibrium of element 2 is expressed by

$$N_3 = (W_2 + S_1)\cos\alpha_5 + N_1\sin\alpha_5 \tag{6}$$

$$S_3 = (W_2 + S_1)\sin\alpha_5 - N_1\cos\alpha_5 \tag{7}$$

where

$$W_2 = \gamma\,[H(aH - L\cos\theta) - \int_{L\cos\theta}^{aH}(x^2/a^2H)dx] \tag{8}$$

Therefore, the total driving force ($S_D$) along the assumed failure surface is

$$S_D = S_2 + S_3 = (W_1 - S_1)\sin\alpha_3 + (W_2 + S_1)\sin\alpha_5 + N_1(\cos\alpha_3 - \cos\alpha_5) \tag{9}$$

The total resisting force ($S_r$) along the failure surface can be expressed as

$$S_F = C'L_2 + N_3\tan\phi'_2 + N'_2\tan\phi'_1 + T_T \tag{10}$$

where

$C'$ = developed cohesion,
$\phi_1'$ = developed friction angle for element 1,
$\phi_2'$ = developed friction angle for element 2,
$N_2' = N_2 + T_N$,
$T_N$ = normal component of the resultant of the axial force in the reinforcing members
$= \Sigma T_i \cos(90 - \alpha_3 - \theta)$,
$T_T$ = tangential component of the resultant of the axial force in the reinforcing members
$= \Sigma T_i \sin(90 - \alpha_3 - \theta)$,
$\Sigma T_i$ = resultant of the axial force in the reinforcing members behind the assumed failure surface (this calculation is described below), and
$L_2$ = length of the entire failure arc, i.e.,

$$L_2 = \int_0^{aH} [1 + (dy/dx)^2]^{1/2} dx$$
$$= (H/2)(a^2 + 4)^{1/2} (a^2H/4) \ln | [2 + (a^2 + 4)]/a^{1/2} | \quad (11)$$

The coefficient $\beta$, the ratio between the normal force and the tangential force at the interface of element 1 and element 2, can then be obtained from the equilibrium of element 2. The driving force in element 2 is $S_3$, and the resisting force can be obtained by using Coulomb's equation.

$$S_3 = C'L_2' + N_3 \tan\phi_2' = (W_2 + S_1)\sin\alpha_5 - N_1\cos\alpha_5 \quad (12)$$

where $L_2'$ = length along the failure arc of element 2, i.e.,

$$L_2' = \int_{L\cos\theta}^{aH} [1 + (dy/dx)^2]^{1/2} dx$$
$$= (H/2)(a^2 + 4)^{1/2} - (L\cos\theta/2a^2H)(a^4H^2 + 4L^2\cos^2\theta)^{1/2}$$
$$+ (a^2H/4) \ln | [2aH + aH(a^2 + 4)^{1/2}]/[2L\cos\theta + (a^4H^2 + 4L^2\cos^2\theta)^{1/2}] | \quad (13)$$

Therefore

$$\beta = 2[C'L_2' + W_2(\cos\alpha_5 \tan\phi' - \sin\alpha_5) + N_1(\cos\alpha_5 + \sin\alpha_5 \tan\phi')]$$
$$\div K\gamma(H - L_1)^2 (\sin\alpha_5 - \cos\alpha_5 \tan\phi') \quad (14)$$

Because $S_1$ cannot be greater than $N_1 \tan\phi'$, $\beta$ must be less than $\tan\phi'$, (i.e., if $\beta < \tan\phi'$, $\beta = \beta$ and if $\beta \geq \tan\phi'$, $\beta = \tan\phi'$).

<u>Case 2: $a < a_T$</u>

A similar expression can be derived for the case in which the failure surface lies entirely within the reinforced soil mass, i.e., when $a < a_T$. For this case,

$$\alpha_3 = \tan^{-1}(L_1/x) \quad (15a)$$

$$\alpha_5 = \tan^{-1}[x\tan\phi/(aH - x)] \quad (15b)$$

The total driving force and the total resisting force developed along the assumed failure surface are expressed in the same manner as for the case in which $a \geq a_T$. The equilibrium equation of element 2 is again used to obtain the ratio ($\beta$) between the normal and tangential forces at the interface of element 1 and element 2.

$$\beta = 2[C'L_2' + W_2(\cos\alpha_5 \tan\phi' - \sin\alpha_5) + N_1(\cos\alpha_5 + \sin\alpha_5 \tan\phi')]$$
$$\div K\gamma(x\tan\theta)^2 (\sin\alpha_5 - \cos\alpha_5 \tan\phi') \quad (16)$$

where

$$L_2' = \int_x^{aH} [1 + (dy/dx)^2]^{1/2} dx$$
$$= (H/2)(a^2 + 4)^{1/2} + (x/2a^2H)/(a^4H^2 + 4x^2)^{1/2}$$
$$+ (a^2H/4) \ln | [2aH + aH(a^2 + 4)^{1/2}]/[2x + (a^4H^2 + 4x^2)^{1/2}] | \quad (17)$$

$$W_2 = H(aH - x)\gamma - \int_x^{aH} (x^2/a^2H)\gamma dx$$
$$= \gamma[(2aH^2/3) + (x^3/2a^2H) - Hx] \quad (18)$$

$$N_1 = (K\gamma/2)(x\tan\theta)^2 \quad (19)$$

## Calculation of Resultant Force in Reinforcing Members

The resultant force of the reinforcing members, $\Sigma T_i$, is the sum of the forces of the individual members. Each force is obtained by calculating the frictional resistance of the portion of the member (its effective length) behind the assumed failure surface. The frictional resistance is the shear stress developed between the reinforcing member and the surrounding soil, i.e.,

$$T_i = \pi D \ell_i (\tau_{ns} + C')/S_H \quad (20)$$

where

$\ell_i$ = effective length of the reinforcing member,
$\tau_{ns}$ = shear stress $= \sigma_n \tan\phi'$,
$\tan\phi'$ = developed frictional coefficient,
$\sigma_n$ = normal stress,
$S_H$ = horizontal spacing of reinforcement,
$C'$ = developed cohesion = C/FS, and
FS = overall factor of safety.

This frictional resistance of each reinforcing member must be smaller than the yield strength of the member; i.e.,

$$T_i < A_s f_y / S_H \quad (21)$$

where $A_s$ = cross-sectional area of reinforcement and $f_y$ = yield stress of reinforcement. From the theory of elasticity,

$$\sigma_n = \sigma_x \sin^2\theta + \sigma_y \cos^2\theta + \tau_{xy} \sin 2\theta \quad (22a)$$

and

$$\tau_{ns} = -\tau_{xy}\cos 2\theta + (1/2)(\sigma_y - \sigma_x)\sin 2\theta = \sigma_n \tan\phi' \quad (22b)$$

Therefore,

$$\tau_{xy} = (1/\cos 2\theta)[(1/2)(\sigma_y - \sigma_x)\sin 2\theta - \sigma_n \tan\phi'] \quad (23)$$

and

$$\sigma_n = \sigma_x \sin^2\theta + \sigma_y \cos^2\theta + \tan 2\theta\,[(1/2)(\sigma_y - \sigma_x)\sin 2\theta$$
$$- \sigma_n \tan\phi'] = (\sigma_y \cos^2\theta - \sigma_x \sin^2\theta)/(\cos 2\theta$$
$$+ \sin 2\theta \tan\phi') \quad (24)$$

where

$\sigma_y = \gamma \bar{Z}_1$,
$\sigma_x = K\sigma_y$, and
$\bar{Z}_1 = Z_1 + (L\cos\theta - x_1)(\tan\theta/2)$
= distance from the ground surface to the center of the effective length (see Figure 6).

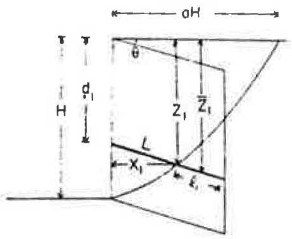


Figure 6. Calculation of effective length of reinforcing members.

$d_i = S_{vi} - S_v/2 \quad (i = 1, \ldots, N)$
$S_v$ = Vertical Spacing
N = Number of Reinforcing Members
$\ell_i = L - X_i/\cos\theta$

$$X_i = \frac{-\tan\theta + \sqrt{\tan^2\theta + 4(H-d_i)/(a^2H)}}{2/(a^2H)}$$

$Z_i = H - X_i^2/(a^2H)$
$\bar{Z}_i = Z_i + (L\cos\theta - X_i)\tan\theta/2$

Figure 7. Typical results of limit analysis.

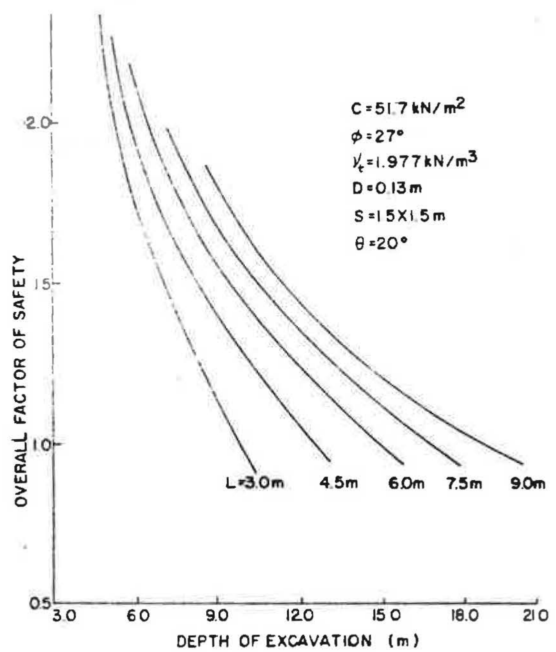


Because the reinforcing members are installed after the excavation, the lower-most member is not considered when the depth of excavation (H) is an exact multiple of the vertical spacing ($S_v$) of the reinforcement. If the depth of excavation is not an exact multiple of the vertical spacing, the number of reinforcing members is assumed to be the integer portion of the $H/S_v$ ratio.

## EVALUATION OF OVERALL STABILITY

The overall stability of the excavation system can be evaluated in terms of Equations 9 and 10. At any stage, the driving force and the resisting force developed along the assumed failure surface must be in equilibrium, i.e.,

$$S_D = S_F \tag{25}$$

The overall factor of safety (FS) is the factor of safety when

$$FS_C = FS_\phi = FS \tag{26}$$

where

$FS_c$ = factor of safety with respect to cohesion and
$FS_\phi$ = factor of safety with respect to friction.

The factor of safety with respect to cohesion (or with respect to friction) is the ratio between the available cohesion (friction) and the developed cohesion (friction), i.e., $C' = C/FS$ and $\tan\phi' = \tan(\phi/FS)$ (if $\phi_1' = \phi_2'$). Because these equations are tedious and because both the driving-force and the resisting-force expressions contain a variable FS term, direct solution is not possible. Therefore, an iterative method was used to calculate the overall factor of safety. The iteration begins by assuming that $FS_c = FS_\phi = L/H$ and then calculates $S_D$ and $S_r$.

A computer program was developed to calculate this overall factor of safety. For a given set of geometric and strength parameters, this program calculates the minimum factor of safety by searching a series of potential failure surfaces passing through the toe of the wall. A typical result of this limit equilibrium analysis for a soil having C = 51.7 kPa and $\phi = 27°$ is shown in Figure 7. The spacings and diameter of the reinforcing members are 1.5x1.5 m and 0.13 m, respectively. The angle of inclination is 20° to the horizontal. The effect of the length of the reinforcing members on the overall stability is shown by the steepness of the curves; the shorter the members, the steeper the curve. For a given depth of excavation, the increase in the factor of safety with increasing reinforcing length is greater when the members are relatively short. For instance, at an excavation depth of 9.0 m, the overall factor of safety increases by 0.35 when the length of the reinforcement increases from 3 to 4.5 m but by only 0.1 when the length of reinforcement increases from 4.5 to 6.0 m. This figure can be used as a stability design chart for calculation of the necessary length of the reinforcing members for a given depth of excavation. It can also be used as a stability analysis chart for estimation of the overall factor of safety of an existing system. Similar charts for different geometries of reinforcement and/or different types of soil can be developed.

## DISCUSSION AND CONCLUSION

The currently available limit-analysis methods (7, 8) for reinforced-earth walls are based on a failure surface consisting of two planes having abrupt changes at the back of the reinforced zone. Because a real failure surface is more likely to be a continuous surface, this analysis uses a parabolic curve to represent the failure surface. The potential failure surfaces predicted by the finite-element analysis and by the limit analysis are compared in Figure 8. The agreement between these two predicted curves is excellent.

Recently, the failure of this system (10) was studied by means of centrifuge model tests. Soil displacements were measured in the model, and maximum shear strain contours were plotted as shown in Figure 9, in which the shaded area indicates the potential failure zone. A limit analysis was also performed for this model, and the shape of the parabolic curve having a factor of safety of 1.0 was computed and plotted on the same figure. That this curve in large portion lies within the potential failure zone strongly supports the validity of the limit-analysis formulation.

The results of the limit analysis were also compared, for a particular example, with the works of Lee and others (4) and Romstad and others (8) (which hypothesize single- and double-plane failure surfaces, respectively). The properties of the example used and the critical

Figure 8. Comparison of predicted potential failure surfaces.

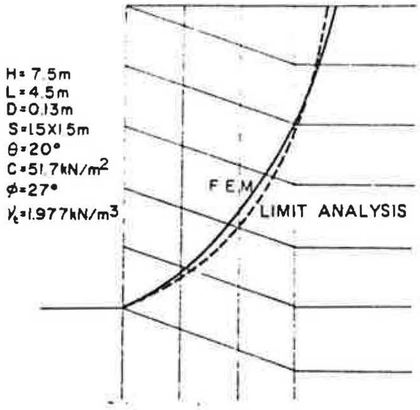


Figure 9. Maximum shear strain contour of centrifuge model at failure.

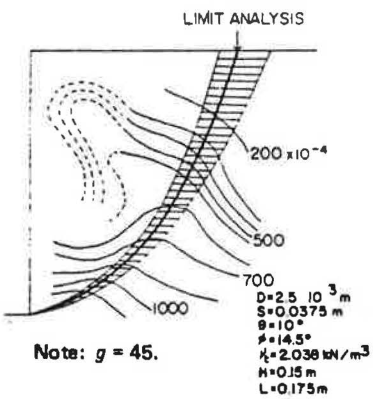


heights of the wall calculated by each method are summarized below:

| Property | Value |
|---|---|
| Cohesion (kPa) | 0 |
| Friction (°) | 36 |
| Unit weight of soil (kN/m³) | 1.96 |
| Diameter of reinforcing bars (cm) | 2.5 |
| Surface area of reinforcing bars (m²/m) | 0.13 |
| Spacing of reinforcing bars (cm x cm) | 60 x 60 |

| | Critical Height (m) | |
|---|---|---|
| Failure Surface | L = 9 m | L = 10.5 m |
| Single plane | 12.3 | 15.3 |
| Double plane | 18.6 | 19.8 |
| Parabolic | 15.0 | 16.5 |

The method proposed by Lee and others predicts the lowest values because it does not consider the development of frictional resistance along the hypothesized failure surface. The double-plane failure-surface assumption predicts the highest critical heights because of the formation of the acute angle near the toe of the wall. The parabolic failure-surface assumption predicts intermediate values (see Figure 10). The differences between the critical heights predicted by either the single- or the double-plane failure-surface assumptions and those predicted by the parabolic failure-surface assumption are approximately 10-25 percent. The less the amount of reinforcement, the larger the difference.

Thus, the proposed limit-analysis method provides a rigorous treatment for the design of a reinforced lateral earth support system for deep excavation.

Figure 10. Comparison of predicted failure heights and surfaces.

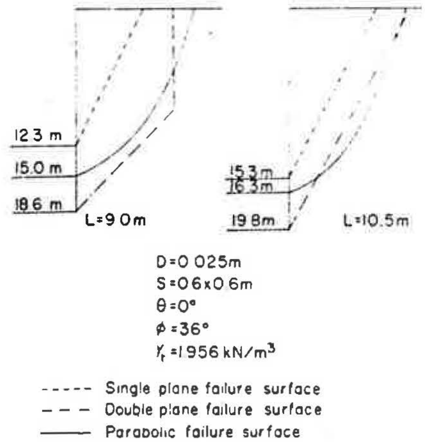


## ACKNOWLEDGMENT

The research reported in this paper was supported by a National Science Foundation grant. We are grateful for this support.

## REFERENCES

1. Sprayed Concrete Wall Cuts Overall Costs by 30 Percent on Underpinning and Shoring. Engineering News Record, Aug. 1976.
2. S. Bang. Analysis and Design of Lateral Earth Support System. Department of Civil Engineering, Univ. of California, Davis, Ph.D. thesis, Sept. 1979.
3. C. K. Shen, S. Bang, L. R. Herrmann, and K. M. Romstad. A Reinforced Lateral Earth Support System. Paper presented at ASCE Spring Convention and Exhibit, Pittsburgh, PA, April 1978.
4. K. L. Lee, B. D. Adams, and J. J. Vagneron. Reinforced Earth Retaining Walls. Journal of the Soil Mechanics Division, Proc., ASCE, Vol. 99, No. SM 10, Oct. 1973.
5. G. Holm and U. Bergdahl. Fabric Reinforced Earth Retaining Walls: Results of Model Tests. Proc., International Conference on Soil Reinforcement, Tokyo, Japan, Vol. 1, March 1979.
6. P. M. Petrick. Laboratory Study of Tensions in Slabs and Deformations of Reinforced Earth Works. Proc., International Conference on Soil Reinforcement, Tokyo, Japan, Vol. 1, March 1979.
7. A. Smith and C. P. Wroth. The Failure of Model Reinforced Earth Walls. Paper presented at ASCE Spring Convention and Exhibit, Pittsburgh, PA, April 1978.
8. K. M. Romstad, Z. Al-Yassin, L. R. Herrmann, and C. K. Shen. Stability Analysis of Reinforced Earth Retaining Structures. Paper presented at ASCE Spring Convention and Exhibit, Pittsburgh, PA, April 1978.
9. L. R. Herrmann. User's Manual for Reinforced Earth Analysis. Department of Civil Engineering, Univ. of California, Davis, Jan. 1978.
10. C. K. Shen, Y. S. Kim, S. Bang, and J. F. Mitchell. Centrifuge Modeling of a Lateral Earth Support. Paper presented at ASCE Fall Convention and Exhibit, Atlanta, GA, Oct. 1979.

*Publication of this paper sponsored by Committee on Embankments and Earth Slopes.*